

CONF-8811100--3

*10  
29079*  
**SANDIA REPORT**

SAND88-2907 • UC-37  
Unlimited Release  
Printed May 1989

*M.L.T.* ①

**The PVDF Piezoelectric Polymer  
Shock-Stress Sensor  
Signal Conditioning and Analysis for  
Field Test Application**

R. P. Reed, J. I. Greenwoll

Prepared by  
Sandia National Laboratories  
Albuquerque, New Mexico 87185 and Livermore, California 94550  
for the United States Department of Energy  
under Contract DE-AC04-76DP00789

*DO NOT MICROFILM  
COVER*

**DO NOT MICROFILM  
COVER**

**MAG**

DISTRIBUTION OF THIS DOCUMENT IS UNLIMITED

## **DISCLAIMER**

**This report was prepared as an account of work sponsored by an agency of the United States Government. Neither the United States Government nor any agency thereof, nor any of their employees, makes any warranty, express or implied, or assumes any legal liability or responsibility for the accuracy, completeness, or usefulness of any information, apparatus, product, or process disclosed, or represents that its use would not infringe privately owned rights. Reference herein to any specific commercial product, process, or service by trade name, trademark, manufacturer, or otherwise does not necessarily constitute or imply its endorsement, recommendation, or favoring by the United States Government or any agency thereof. The views and opinions of authors expressed herein do not necessarily state or reflect those of the United States Government or any agency thereof.**

---

## **DISCLAIMER**

**Portions of this document may be illegible in electronic image products. Images are produced from the best available original document.**

Issued by Sandia National Laboratories, operated for the United States Department of Energy by Sandia Corporation.

**NOTICE:** This report was prepared as an account of work sponsored by an agency of the United States Government. Neither the United States Government nor any agency thereof, nor any of their employees, nor any of their contractors, subcontractors, or their employees, makes any warranty, express or implied, or assumes any legal liability or responsibility for the accuracy, completeness, or usefulness of any information, apparatus, product or process disclosed, or represents that its use would not infringe privately owned rights. Reference herein to any specific commercial product, process, or service by trade name, trademark, manufacturer, or otherwise, does not necessarily constitute or imply its endorsement, recommendation, or favoring by the United States Government, any agency thereof or any of their contractors or subcontractors. The views and opinions expressed herein do not necessarily state or reflect those of the United States Government, any agency thereof or any of their contractors.

Printed in the United States of America. This report has been reproduced directly from the best available copy.

Available to DOE and DOE contractors from  
Office of Scientific and Technical Information  
PO Box 62  
Oak Ridge, TN 37831

Prices available from (615) 576-8401, FTS 626-8401

Available to the public from  
National Technical Information Service  
US Department of Commerce  
5285 Port Royal Rd  
Springfield, VA 22161

NTIS price codes  
Printed copy: 03  
Microfiche copy: A01

# **The PVDF Piezoelectric Polymer Shock-Stress Sensor**

## **Signal Conditioning and Analysis for Field Test Application**

**SAND--88-2907**

**DE89 013348**

R. P. Reed and J. I. Greenwoll  
Field Measurements Division  
Sandia National Laboratories  
Albuquerque, NM 87185

### **Abstract**

The PVDF shock sensor is a piezoelectric polymer transducing element that converts stress to charge. This unusually versatile sensor allows accurate measurement of stress pulses of durations up to milliseconds with resolution of nanoseconds over a range of a few bars to at least 0.5 Mbar. Its measurement characteristics depend significantly on stress waveform and circuitry. Field test applications require special consideration of signal conditioning, system characterization, and data analysis. This report describes some unfamiliar characteristics of the PVDF sensor and a field-validated hybrid (complementary hardware and software) approach to the general measurement problem as encountered under field test conditions. Discussed are the use of the sensor, from estimation of signal voltage, through characterization and correction for system properties, design, and realization of special filters, to reduction of observed voltage to the stress experienced by the sensor.

---

Presented at the Fifth State-of-the-Art Blast Instrumentation Meeting, Defense Nuclear Agency Test Directorate, Kirtland Air Force Base, Albuquerque, NM, 15-16 November 1988.

## **Acknowledgments**

The authors sincerely appreciate the indispensable support of Steve Breeze and Perry Jones, Sandia's Division 7116; Stan Dains and the fielding personnel of 7120; and the invaluable technical contributions of R. A. Graham, 1131; Larry Lee, David Fogelson and staff, Ktech Corp.; and Dr. François Bauer, French-German Institute of Saint-Louis, France (ISL).

# Contents

Introduction .....	7
Piezoelectric Application Modes .....	9
Mechanically Determined Modes .....	9
Electrically Determined Modes .....	9
System Characteristics .....	12
Numerical Integration .....	12
Hardware Integration .....	13
Imperfect Integrators .....	15
Measurement System Response .....	16
Hybrid Integration .....	16
Signal Prediction .....	17
Example of Prediction and Deduction .....	17
Prediction of Output Voltage .....	17
Reduction of Recorded Voltage to Stress Input .....	18
Significance of Example .....	20
Summary .....	21
References .....	21
APPENDIX—Numerical Methods .....	23

## Figures

1 Sandia standardized PVDF shock-stress-sensing element .....	7
2 Special shock-stress gauge assembly using a $1 \times 1$ -mm PVDF sensor element for in-material stress measurements .....	8
3 Mechanically defined piezoelectric gauge application modes .....	9
4 Some selected calibration data for $3 \times 3$ -mm Sandia standard PVDF shock-stress sensor elements .....	11
5 Generalized equivalent circuit for stress-wave measurements by piezoelectric sensing elements .....	11
6 Elementary quasi-integrating hardware circuits .....	13
7 Time-domain response of a hardware integrator .....	14
8 Waveform conversion from stress to charge to voltage .....	18
9 Voltage step response characteristics of the measuring system and its hardware and numerical components .....	19
10 Calculated input stress deduced from “recorded” voltage .....	20

## Table

1 Calibration data for $3 \times 3$ -mm PVDF stress sensors of the Sandia standard design .....	10
---	----

# The PVDF Piezoelectric Polymer Shock-Stress Sensor

## Signal Conditioning and Analysis for Field Test Application

### Introduction

Polarized polyvinylidene fluoride polymer film (abbreviated as PVDF) can be used as the active material for an accurate self-generating piezoelectric stress sensor.<sup>1,2</sup> Sensing elements are usually about 25  $\mu\text{m}$  (1 mil) thick and have a sensing area of less than 1 to more than 25  $\text{mm}^2$ . The sensor has an exceptional stress range of use—from the acoustic range to as much as half a megabar. Transient stresses with rise times of nanosecond order can be resolved. The duration of loading may be as long as milliseconds, limited by the experiment design and not by the gauge element.

The simple homopolymer, PVDF, is formed from the vinylidene fluoride monomer  $[-\text{CH}_2-\text{CF}_2-]$ ; therefore, it is a low-Z material with no element of atomic number higher than 9 (H=1, C=6, F=9). Electrodes are gold over platinum, less than 0.1 nm thick. PVDF is suitable for use in typical radiation environments of nuclear testing. PVDF sensors have been used successfully in both x- and neutron-radiation environments, but general limits of accept-

able exposure have not been well established. The polymer material is of a special measurement grade. The raw material pellets can be extruded and bilaterally stretched to yield a film of <10 to >200  $\mu\text{m}$  thick. In this form, it is polycrystalline with its crystal structure oriented to allow it to be piezoelectrically polarized.

For making measurement-grade shock-stress sensors, the polarization must be accomplished by a proprietary cyclic poling process specially developed for this demanding application.<sup>3</sup> Evolved and proved over a period of several years, this process eliminates several extraneous charge-release mechanisms that would produce spurious and erratic responses under shock-loading conditions.

The flexible and tough material can be fabricated in widely different forms and sizes. For shock-stress measurements in laboratory and field applications, Sandia Laboratories has developed a standard geometry for shock-sensing elements, shown in Figure 1. A formal specification document is being prepared to detail the essential features of the sensing element.<sup>4</sup>

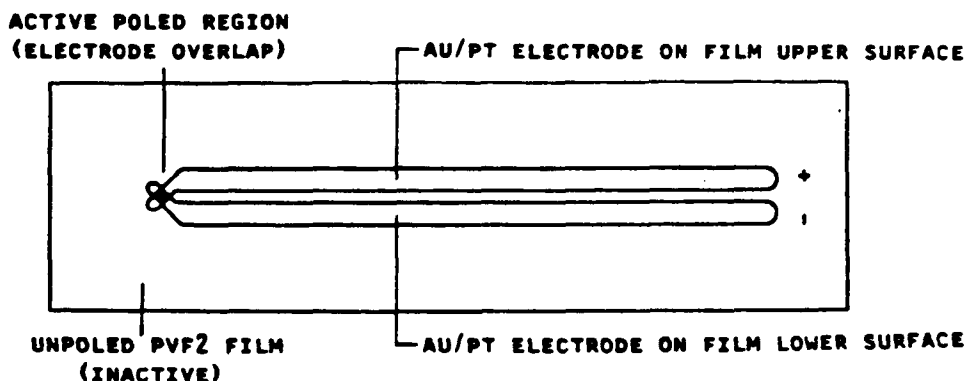


Figure 1. Sandia standardized PVDF shock-stress-sensing element

The Sandia geometry evolved from the original design of François Bauer of the French-German Research Institute of Saint-Louis, France.<sup>1</sup> Gauge elements of this standard configuration and of comparable material are now commercially available.<sup>5</sup>

PVDF shock-stress elements produced by processes, from materials, and to dimensions other than those required by the Sandia standard may have significantly different response, reproducibility, and accuracy and, under some circumstances, may exhibit spurious response.

A sensing element is formed by sputtering thin-film electrodes on opposite faces of PVDF film so that a square area is formed where the opposing electrodes overlap. The electrodes, ~0.1 nm thick overall, are made of gold over a thin bonding layer of platinum. An electrical potential is applied between the leads to produce an electrical field of several hundred volts per micrometer only in the square region where the electrodes overlap. This region alone becomes polarized and is the active area of the sensor. The remainder of the film is inactive and does not shock-polarize. Teflon film is used to insulate the PVDF element in order to avoid shock-induced polarization at high stress.

In this polarized configuration the poling direction normal to the thickness of the film is designated as the 3-polarization axis. The two in-plane directions of stretching are the 1 and 2 directions. The three axes are mutually perpendicular. The specific charge (the charge per unit of active electrode area) resulting from a change of stress or temperature state is collected from the electrodes along the 3 direction. Generally, this specific charge is:

$$Q_3/A = d_{31} \sigma_1 + d_{32} \sigma_2 + d_{33} \sigma_3 + \pi \Theta \quad (1)$$

where the  $d_{ij}$  are piezoelectric coefficients expressing charge produced from normal stress in the three directions, the  $\sigma_i$  are changes in normal stresses in the three directions, and  $\pi$  is the pyroelectric coefficient that expresses the charge response to any scalar temperature change,  $\Theta$ . Because the necessary crystal orientation is produced by stretching,  $d_{31}$  and  $d_{32}$  are not necessarily identical. For this material and electrode configuration, there is ideally no response to shear stresses. A sensing element can produce only one scalar response to any combination of the four possible measurands. For measurement, either three of the measurands must be suppressed by experiment design or else those that change during measurement must vary in a consistent and known way as in planar impact experiments. The simplest response is for the constant temperature hydrostatic stress state where the three normal stresses are identical (i.e., pressure).

The PVDF sensor is standardized and characterized separately as a transducing element, analogous to a strain gauge, rather than as a gauge assembly. The PVDF sensing element is only one essential component in a stress-measuring gauge assembly. The gauge assembly, in turn, is only a part of a measurement system. It is the responsibility of the user to ensure that the well-characterized transducing element is exposed to stress-loading states corresponding to calibrations and to appropriate signal conditioning in a measurement.

An example of a PVDF element assembled into a special gauge assembly to measure in-material shock stress under severe field conditions is shown in Figure 2. This application is typical of the many diverse uses of the PVDF sensor element in field-testing where the gauge assembly is not general-purpose but, rather,

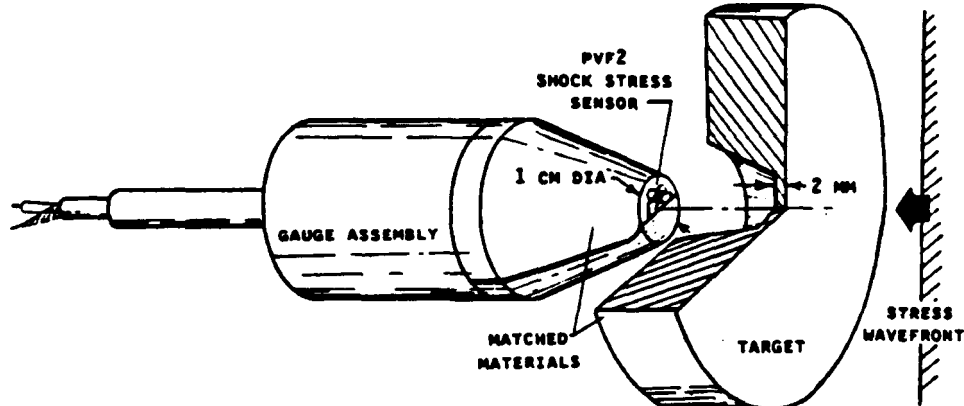


**Figure 2.** Special shock-stress gauge assembly using a 1×1-mm PVDF sensor element for in-material stress measurements

must be tailored to address the objectives of the specific measurement.

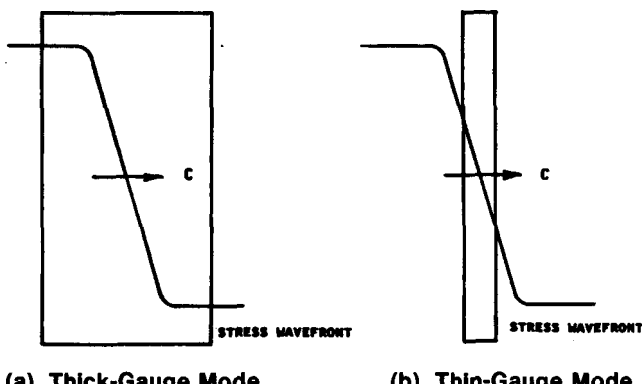
## Piezoelectric Application Modes

The characteristic voltage response of any piezoelectric sensing element is governed by both mechanical and electrical circumstances and not by the sensor alone. Although the relation between stress and charge in the sensor is the same in all circumstances, the observed output voltage response depends on the nature of both the stress pulse and the recording circuit.

### Mechanically Determined Modes

#### Thick-Gauge Mode

A piezoelectric element subjected to an abrupt propagating stress pulse that rises to a plateau over a distance less than the thickness of the active element, Figure 3(a), produces an output that is a function of the stress difference between the two faces of the sensor.<sup>6a</sup> Therefore, for the period until the stress front arrives at the quiescent rear surface of the sensor, the element responds to the front-surface stress history.



(a) Thick-Gauge Mode

(b) Thin-Gauge Mode

**Figure 3.** Mechanically defined piezoelectric gauge application modes

In the traditional name for this application mode, the *thick-gauge mode*, thickness is relative to the stress pulse rise time. Both the classic Sandia Quartz Shock-Stress Gauge<sup>6a</sup> and the Sandia Field Test Shock-Stress Gauge<sup>6b</sup> are used in this mode and are limited in measurement duration by the thickness of the gauge element. This limits use to the transit time of the wave through the element (about 1.7  $\mu$ s per centimeter of thickness, less than 3.3  $\mu$ s total in most

quartz gauges). In contrast, the transit time through the 25- $\mu$ m PVDF gauge is on the order of only 10 ns. But, during this brief interval, the PVDF element behaves like, and has been used in much the same way as, the thicker sensors for special high time-resolution measurements.

#### Thin-Gauge Mode

If the gage element is subjected to a wave that rises to crest over a distance many times the thickness of the sensor, Figure 3(b), the element progressively approaches equilibrium through wave reverberation. Subjected to a stress step pulse, equilibrium is essentially attained in 5 to 10 wave transit times. In the equilibrium state, the sensor effectively responds to the average stress over the element's active volume. For a 25- $\mu$ m element, the limiting response is on the order of 50 ns. For most field applications, this *thin-gauge mode* is employed because rise times are relatively slow, on the order of several microseconds or milliseconds in duration.

Paradoxically, a *thick* gauge can resolve faster rise times but with limited duration whereas a *thin* gauge can monitor pulses of longer duration but with slightly reduced time resolution.

#### Stress and Temperature State

As shown by Eq. (1), the response of the sensing element depends not only on the magnitude of stress but also on its tri-axial state and on the possible variation of temperature during the period of measurement. The possibility of hysteresis, a difference of response on loading and unloading, is not addressed here. In calibrations to date, the hysteresis appears to be small for PVDF sensors. As is true for any stress-transducing element, the PVDF sensing element can be used for accurate measurement only under particular mechanical conditions for which appropriate calibration is available.

### Electrically Determined Modes

Two electrically determined application modes are called the *charge mode* and the *current mode*, depending on whether the voltage is measured in the capacitive-shunted "open-circuit" or in the resistive-shunted configuration. The dynamic behavior between these two extremes of electrical load is not ordinarily useful for measurement; however, the successful hybrid measurement technique described below does effectively use the response in an intermediate mode.

The PVDF stress element is used in either of the two modes depending on the requirements of the

particular experiment. Each produces for measurement a usable but quite different voltage response that must be interpreted in an appropriate way. If care has not been taken to characterize and to record definitely in one mode or the other by proper attention to these circuit considerations, creative data analysis by the experimenter may rationalize but cannot salvage the meaningless data.

### Piezoelectric Conversion

Both charge and current modes begin with the same stress-to-charge piezoelectric conversion. Shock-stress elements are usually destroyed by calibration; therefore, all sensor elements must be highly reproducible to a standard characteristic in order to allow accurate use. Individual PVDF sensors cannot be nondestructively calibrated to improve accuracy at high stress because low-stress measurements do not adequately characterize high-stress behavior.

Calibration of standardized PVDF sensor elements has been conducted over a broad range of stresses.<sup>7</sup> Calibrations to date have related principally to the specific polarization or charge per unit area versus shock stress in a one-dimensional strain state. The calibration subjects were fabricated in three different laboratories in France and in the US. All were fabricated by the same standardized process using special PVDF measurement-grade films. They ranged in active area from 1 to 25 mm<sup>2</sup>. The calibration stress levels have ranged from less than 1 bar to 460 kbar. Calibrations conducted in different gas gun facilities and by shock tube have been consistent between sources, gauges, and laboratories. The degree of agreement has justified the preparation of a generic calibration for standard PVDF sensor elements.

The authorized calibration will soon be released by Sandia at the completion of the study.<sup>7</sup> For now, Table 1 presents a few calibration data points for one sensor configuration measured in one facility. These data are a small subset for one kind of sensing element from many tests of different kinds of elements.

The data are for typical elements of a 9-mm<sup>2</sup> area for stresses from 10 to 160 kbar (Ref. 8). The calibration of gauges of this size and design that are commercially available from the French manufacturer is also well described by this data.<sup>5</sup>

These few data points can be usefully represented by the two-parameter power-law relation:

$$\frac{Q}{A} = 0.328 (\sigma^{0.546}) \quad (2)$$

where stress is in kilobars and polarization is in microcoulombs per square centimeters. The function is represented graphically in Figure 4. This objective least-squares fit is arbitrarily of the same form used by Bauer in reporting his first calibrations of PVDF gauges of different types.<sup>1</sup> The power-law form is particularly convenient for both output prediction and reduction of experimental data.

**Table 1. Calibration data for 3×3-mm PVDF stress sensors of the Sandia standard design** [From Ref. 7]

Shock Stress*	Specific Charge μC/cm <sup>2</sup>
0.0	0.0
3.09	0.376
7.32	0.774
26.1	1.96
45.0	2.76
93.1	3.99
160.0	5.15

\*Loading imposed by projectile impact resulting in transient one-dimensional strain state of stress.

The power-law form is not necessarily suggested by physical considerations and does not adequately represent this particular data set for peak stresses lower than 10 kbar. This convenient temporary relation is adequate for the prediction and data reduction of Sandia standardized gauges for peak shock stresses of 10 to 160 kbar until the standard calibration is released.

The eventual standardized calibration relation, which will depend on the selective grouping of data from different experimenters, laboratories, and gauges, may differ from this temporary curve and might be of a different form.<sup>7</sup> The calibration, Eq. (2), will not generally apply to PVDF sensors of material, thickness, or fabrication that are different from the standardized gauge.

### Piezoelectric Response

The basic piezoelectric transduction process converts a change of stress to a change of charge. The relation of the time variation of this charge to the observed output voltage is dictated by the measurement circuit chosen. A generalized equivalent circuit of the piezoelectric sensor and associated measurement components is shown in Figure 5.

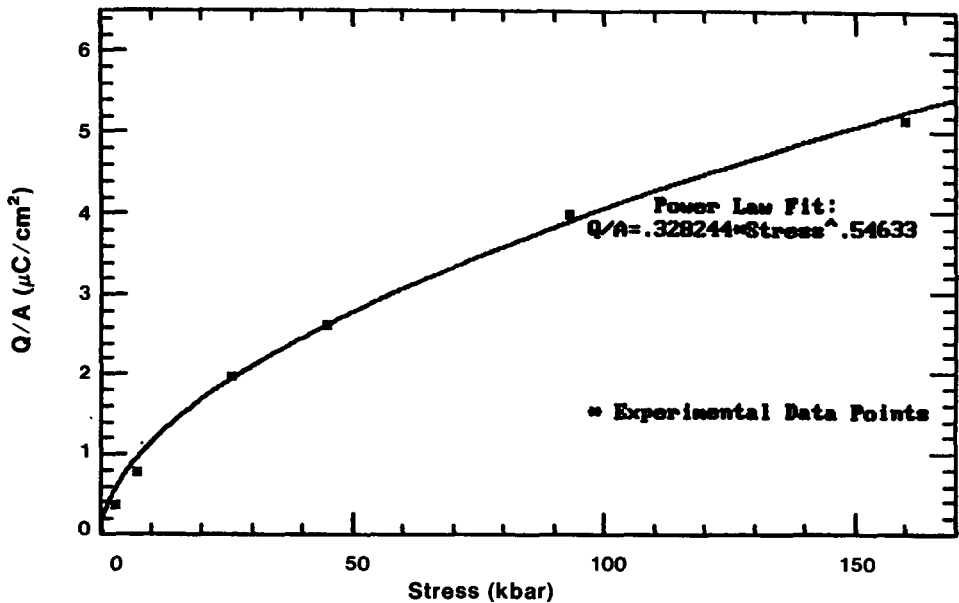


**Figure 4.** Some selected calibration data for 3×3-mm Sandia standard PVDF shock-stress sensor elements. PVDF gauges are usable to at least 460 kbar.

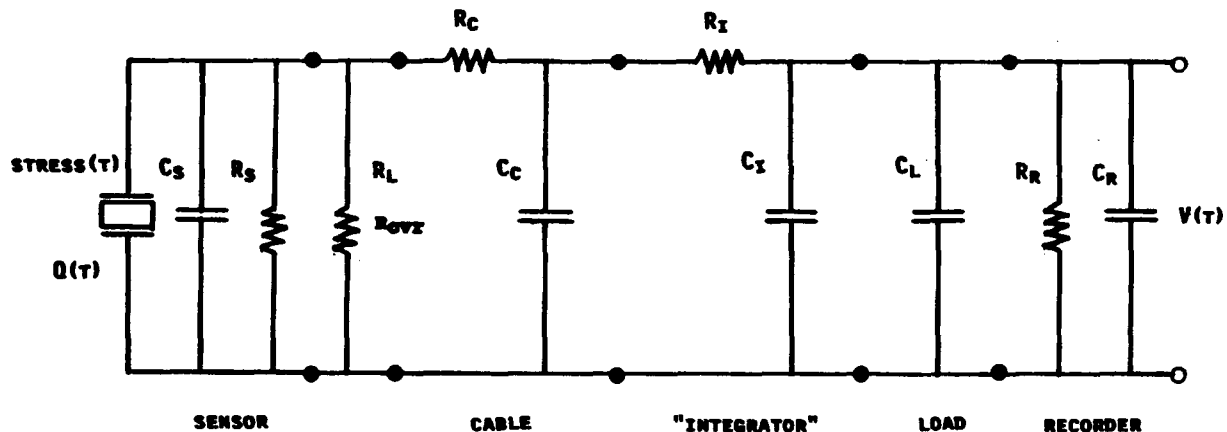


**Figure 5.** Generalized equivalent circuit for stress-wave measurements by piezoelectric sensing elements

The simplified circuit is schematic in representing sections of distributed parameter values as discrete components. The distinction between lumped and distributed parameters is important in actual transient response. Different modes are related to different relative values of circuit parameters. The schematic depicts the sensor, cable, signal conditioning, recorder, and alternate load components across which the output voltage can be observed. The circuit is typical of those used in field recording. Circuit components can take on a wide variety of values that define the measurement response mode.

### Charge Mode

Where the load resistance,  $R_L$  shunting the sensor is very large ("open circuit"), a constant stress state of

the sensor corresponds to a constant charge state. The voltage is observed across the load capacitor indicated as the lumped value,  $C_L$ .

For operation in this mode the load impedance must be very high, often greater than  $10 \text{ M}\Omega$ . A stable op-amp voltage-follower circuit may be used to accomplish this condition. Where the load resistance is large, the steady-state charge is distributed between capacities of the sensor, the connecting cable, measuring system components, and the voltage-viewing load capacitor. The open-circuit voltage across the capacitor is a measure of charge and so, indirectly, of stress. The capacitively loaded "open circuit" functions as a capacitive charge divider.

This mode is susceptible to noise induced by spurious charge and to capricious changes of capacitance in the transmission line. Nevertheless, in special circumstances in the field, this mode has been used successfully with high signal-to-noise ratio because of the high-level signals generated by the PVDF sensor.

### Current Mode

Where the sensing element is shunted by a small resistance, the charge from the gauge element flows through the resistor as a current. The voltage drop across the known current-viewing resistor (CVR),  $R_q$ , is a measure of that current, thus of the change of charge and so, even more indirectly, of the stress.

## System Characteristics

Beyond the stress transducer, the transmission line, filters, signal conditioning, and recorders distort the voltage that is output by the sensor. These regular transient response characteristics can all be lumped into a single "transfer function" that may be represented as the step response of the overall system. The stress measurement response is the response of an entire system, of which the sensor is merely a part.

### Transmission Line

In field measurements, transmission lines are often several hundred meters in length. Long cables not only introduce signal delay and steady-state attenuation but they also tend to distort the signals they transmit. The specific distortion of the particular cable to be used for measurement is most easily characterized by introducing a known step function voltage pulse at the gauge end and recording the output at the recording end. This one quick experiment captures both amplitude and phase characteristics of the cable in a manner best suited to field operations.

### Recorder

In field measurements, the bandwidth fidelity (either high or low frequency or both) is often marginal for the waveforms to be recorded; therefore, it is essential to include the recorder and associated preamps in transient system characterization.

### Integrator

Where the sensor is used in the current mode, the voltage is, to a degree, representative of the derivative of the nonlinearly scaled stress measurand. The actual stress waveform that corresponds to the observed voltage waveform must be determined by a process

that includes both mathematical integration and nonlinear scaling. Therefore, to complete a measurement recorded in the current mode, an integration must be performed either numerically or electrically.

### Integration Methods

Integration of the voltage waveform to deduce sensor charge may be accomplished by approximate numerical or electrical means. Familiar methods for numerical differentiation and integration are summarized in the Appendix. Neither electrical nor numerical processes are exact. Careless application of either method can result in errors ranging from insignificant to extreme.

## Numerical Integration

Because a result of numerical integration (quadrature) is approximate, except in unusual circumstances, it is always appropriate in stating results of data reduction to specify the time step and method used for the operation. One prominent form of error in numerical integration results from random amplitude bias error in the sampling process. Each amplitude of an experimental waveform is approximated with some systematic bias and some random uncertainty. Where a waveform is sampled, each resulting number may be in error by a discrete amount that depends on the resolution of the digitizing method or the number of digits used to report it. This is sometimes called a *bin-* or *bit-toggling* error.

The effect of sampling error on the integration result is most evident in the treatment of slightly noisy segments of the waveform that are at nearly constant amplitude as on baselines or on the plateaus of square pulses. The effect is necessarily introduced in the sampling of a voltage amplitude that is near constant but does not remain within a single discrete sampling level.

Depending on the relative position of each near-constant level within the bit-toggling level of sampling, a progressive integral of the waveform can produce an integrated waveform that is "tilted." Even very slight baseline offsets that are not visually apparent in the raw function are readily apparent in its integral. This problem is familiar to those who have integrated accelerometer data to yield either velocity or displacement.

Such data is often corrected for the obvious "tilt" of the integral that is evident from the integration of a baseline that precedes an arbitrary waveform. It is important to make this persistent correction; but, it should be recognized that the correction value at each level is generally different and cannot be known. The effect is present but not evident and is of less effect in

waveform segments of continually changing amplitude. An effect of simple baseline offset is persistent, obvious, and is simply added to any other effects.

Other strictly mathematical errors of numeric integration are classic and are described in many references on numerical methods of analysis.

## Hardware Integration

One signal-conditioning component that immediately appears to be useful as applied to current-mode recording is a hardware integrator. One motive for using the integrator is to produce a voltage signal that resembles the stress input rather than the derivative of stress. However, there are reasons that both favor and disfavor such usage.

Although its electrical response characteristics are simple and well known, the classic "low-pass RC first-order filter" electrical "integrator" is superficially described in typical incidental treatments. For this reason, hardware integrators are often misunderstood and misused. It is commonly and correctly stated that for the simple low-pass RC filter shown in Figure 6(a) that

$$V_{\text{out}} = \frac{1}{RC} \int_0^t V_{\text{in}} dt. \quad (3)$$

The inverse RC "time constant" appears as a scaling multiplier. Although Eq. (3) is conditionally true, this simplistic treatment ignores some important facts having a great effect in transient measurement.

A practical (from a mathematical perspective) definition of a hardware integrator is: a filter that when subjected to a strict voltage step input, Figure 7(a), responds with a strict linear ramp voltage output, Figure 7(b). This is an appropriate test for the

adequacy of any integrator. Though the simple first-order low-pass RC filter is commonly described as an integrator, the response of even an ideal classical "RC integrator" does not literally fulfill this practical definition.

For a step input of voltage, the output of the ideal first-order RC integrator is:

$$V_{\text{out}} = k [1 - \exp(-t/\tau)] V_{\text{in}} \quad (4)$$

where,  $\tau$ , the product of resistance and capacitance, is the classic "time constant" of the first-order filter and  $k$  is related to  $1/\tau$ , Figure 7(c). Thus, the "integrator" response to a step is never truly a linear ramp; therefore, it is never rigorously an integrator. It can, however, acceptably approximate a linear-ramp integrating characteristic for some initial time interval. The circuit can serve as a practical integrator, but only for a limited duration of observation, Figure 7(c).

For example, the step response is within about 2% of a linear ramp for any duration less than one-tenth the integrator time constant, but the response very rapidly deviates from the ideal integrating characteristic as the duration of recording increases. In practice, this characteristic limits the use of the hardware integrator for long duration pulses.

In principle, by choice of time constant, the integrator may have any desired integrating duration. In practice, the available size of the hardware capacitor is limited and the reciprocal RC product imposes an attenuation that may not be acceptable. The amplitude of response is inverse to the time constant. Long integration times are accomplished with a corresponding loss of signal amplitude.

Because of distributed capacitance and inductance, the real hardware integrator may also have a gradually increasing "toe" that causes distortion and effective delay through the filter, Figure 7(d).

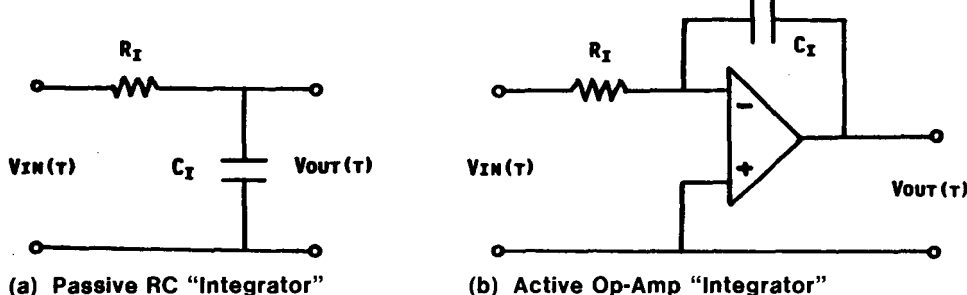


Figure 6. Elementary quasi-integrating hardware circuits

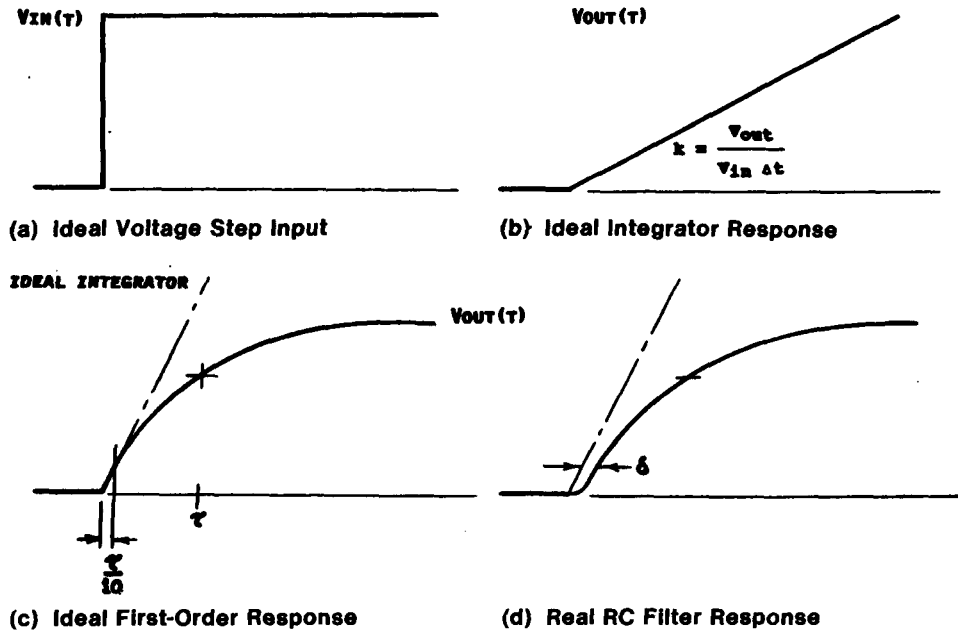


Figure 7. Time-domain response of a hardware integrator

### Active Integrators

The passive RC filter is convenient because it requires no power supply, but it is also limited in its capabilities. Active integrators, Figure 6(b), based on operational amplifiers are more complex and require powering. But, in a powered integrator, desirable stages of impedance-matching and amplification can precede the integration and a line-driving stage can follow the integrator where the signal must be conveyed over long distances. This is the principal benefit of active integrators.

However, active IC integrators are limited in time constant in long-term response in the very same way as the passive filter. They may further limit the response slew rate and maximum voltage excursion of the recordable input. Also, they may increase the noise level. More complex active IC integrating circuits are possible. They can allow the integrating duration to be extended by using electrical components of practical values. A preferred alternate approach to hybrid hardware-software integrators combining passive filters and numerical filters will be described below.

### Integrator Scaling

The physical dimensions of an integrated waveform are in units of volts-time. A hardware integrator represents these physical units simply as a voltage output that must be scaled to deduce the input. Although the scaling is theoretically related to the time constant, in hardware integration there are other

losses. Also, the duration of linearity relative to the time constant modifies the effective scaling factor. Therefore, practical scaling for measurement is determined by imposing an accurate voltage step input of adequately short rise times, flat crest, and known amplitude, and observing the nearly-linear ramp output. The simple and practical measured scaling multiplier in the ideal circumstance is:

$$k = \frac{V_{\text{out}}(t_{\text{max}})}{t_{\text{max}} V_{\text{in}}(t_{\text{max}})} \quad (5)$$

where  $t_{\text{max}}$  is the required duration of recording. Unfortunately, for the real imperfect integrator in which the response is not essentially a linear ramp, Figure 7(d),  $k$  is not a constant. A simple constant multiplier cannot be used, nor can a variable multiplier. The "integrating" conversion must be performed by conventional convolution, as will be described.

### Advisability of Using a Hardware Integrator

#### Laboratory Applications

Obviously, a hardware "integrator" should never be used blindly as a black-box component. It can unexpectedly distort the signal. It must be appropriate for the waveform. In the laboratory, where waveforms can be predicted well, where signal lines can be short, simple, and of excellent quality, and where signal-to-noise ratios can be controlled, the use

of hardware integrators is rarely desirable. Under these ideal conditions, the PVDF sensor should usually be used in the current mode because of the possibility of greater accuracy and much finer time resolution. This approach, used under highly controlled conditions, reveals quite different data-reduction problems than those encountered in field use.<sup>9</sup>

A hardware-integrated result is no different in principle than that from recording directly in the charge mode operating into a high-impedance load. If the objective is merely to obtain a record that is representative of the charge, the introduction of an RC integrator is a superfluous complication. A voltage-follower operational amplifier circuit that provides a high-input impedance is best suited to this application, but may limit the measurements in slew rate and amplitude range.<sup>6c</sup>

Although they give the appearance of simplification, hardware integrators introduce errors and opportunities for gross misuse. They eliminate only one simple and straightforward step of the data-reduction process, usually at a sacrifice to accuracy. They should not be used where the most accurate measurements are expected.

Also, the hardware-integrated result does not produce a direct representation of the stress waveform because additional analysis is still required to remove the distortion that results from the nonlinear relation between stress and voltage.

## Field Test Applications

There are, nevertheless, many circumstances in field measurement where some form or approximation of hardware integration is appropriate for signal-conditioning PVDF stress sensors. Conditions that suggest hardware integration may be desirable include:

- Poorly predicted waveshape
- Indefinite maximum stress rate
- Very short rise time stress pulse
- Long electrical cables
- Barely adequate, high-frequency recording capability
- Marginally acceptable time-sampling resolution
- Inadequate amplitude "bit" resolution
- Single-channel recording without backup

Most of these conditions are common in field applications.

On the other hand, in another common circumstance—slow-rising, long-duration pulses—it is often necessary to record without a hardware integrator because signal amplitudes may be inadequate

or physical components for long-duration integration may be impractical.

Current-mode operation is usually preferred for use in the field to reduce the substantial effect of noise. In current-mode recording the observed voltage is somewhat proportional to the local stress *derivatives* rather than to stress *values* of the measurand waveform. The voltage waveshapes are markedly different in charge- and current-mode recording. This simple fact is of immense practical importance, yet its significance is frequently not recognized.

In many common calibration and application situations, when the stress is at a very high peak or plateau value, the sensor output is *zero!* Peak output voltage cannot be directly predicted simply from the peak stress; stress rate must be used.

The practical significance of this point in experiment fielding cannot be overemphasized. Often, the major feature in the current-mode record is an inconspicuous feature of the stress waveform. In current-mode recording, it is the maximum *stress rate* rather than maximum *stress value* that determines the greatest voltage amplitude to be recorded.

Unfortunately, subtle features of the stress waveform are the most difficult to calculate accurately. This complicates the prediction of the voltage range that must be recorded. Slight variations in seemingly insignificant features of the stress waveform can result in greatly different voltages in the current-mode output. A reliable choice of scale for recording may be difficult. The best compromise between definite capture of signal and adequate bit resolution may not be apparent in preparing to record a field experiment.

Proper hardware integration for field recording can make the prediction of voltage output signal much more reliable by reducing the sensitivity of response to uncertainties of prediction; thus, integration can often improve the chance of successful data capture. Also, in field operations, the bandwidth of available recorders is sometimes barely adequate. The bandwidth required to record the derivative is about double that required to record the stress function itself; therefore, hardware integration can reduce the recording bandwidth requirement by a factor of 2 or more. This is another benefit of hardware integration.

## Imperfect Integrators

Real hardware integrators are limited not only by their late-time response, as suggested above, but also by their high frequency response. At higher frequencies, the effective circuit of the integrator must include distributed inductive and capacitive elements that produce a "toe" in the step response and a

persistent offset from the ideal ramp, Figure 7(d). It must be ensured experimentally that such effects are not significant for the specific waveform of interest. A hardware integrator is not a magic black box that produces a proper integral as output regardless of the input waveform. It must be matched to the application, confirmed, and calibrated for that use.

## Measurement System Response

In all dynamic measurements, careful experimenters consider the effect of actual system response on the data. The system transfer function that includes the effects of the transmission line, amplifiers, recorders, terminations, and impedance discontinuities, as well as any "integrator," must effectively be involved in data analysis. For transient stress measurements under field conditions, and also in the laboratory, these factors very often are significant.

Long transmission lines distort the signal, signal lines may be composed of several dissimilar cables in series, the cable may be imperfectly matched at the source or recording ends (causing reflections), and signal-conditioning components may distort the waveform. The simple "dc step cal" even when conducted at multiple levels to document dc linearity is inadequate for transient measurement.

Even where system response is believed to be adequate, such system step characterization is necessary to confirm and document an adequacy that may be presumed. A characterizing step voltage input of rise rate that is much less than the maximum stress rate and duration longer than the cable reflection time and duration of measurement is essential as a quantitative documentation of the system. In such characterization, except for reflections, the sequence in which components are placed in the system is not important. For example, an integrator may be placed at either the source or receiving end of the signal line or at any intermediate point.

## Hybrid Integration

To address the general problem of marginal system response and an imperfect integrator, we have used a complementary numerical filter—an imperfect hardware integrator combined with a complementary digital compensating filter we call a hybrid integrating filter. Such a filter can be used to complete integration performed inadequately by a hardware "integrator" and concurrently to compensate for other system distortion. In this instance, the hybrid filter replaces the cable equalizing filter that is often used to correct for cable distortion.

The ordinary mathematical operation of convolution and its inverse, deconvolution (see the Appen-

dix), can be viewed simply as filtering operations. Like integration, these operations can be performed numerically as well as by hardware.

Passive hardware filtering performed during recording can only selectively attenuate appropriate frequencies in the distorted signal; therefore, any passive hardware filter is used with a loss-of-signal level and usually of signal-to-noise ratio. These losses are not experienced with numerical filters.

Numerical filters are applied to the data after recording. Obviously, if the data are not successfully captured or if they are recorded with inadequate resolution, numerical filtering cannot be fully successful. Where the desired output of a system is the integral of the input, it is appropriate in the hardware filter to attenuate from the distorted signal only those frequencies that further that objective.

Numerical filters are much more easily realized for correction functions of arbitrary waveform than are hardware filters. The data required to design a compensating filter is merely a measured step-function response of the overall recording system that includes the imperfect integrator. The step-response characterization captures, adequately and simply, both the amplitude and the phase characteristics of the actual "transfer function" of the system.

Most of the benefits of integration required to allow reliable recording of a poorly predicted stress input can be obtained with a very simple, though imperfect, hardware "integrating" filter. In some instances this may consist of no more than a capacitor of appropriate value that shunts the recorder, as in charge-mode recording, using the incidental resistance of the signal cable to determine the "integrator" time constant. This generally produces a predictable and recordable waveform, with confidence and with acceptable attenuation, but one that is also significantly distorted.

In the hybrid approach, the overall system, including the integrator, is characterized by a voltage-step pulse. The ideal linear ramp waveform of the desired integrator is then deconvolved with the overall system response waveform in order to deduce the necessary waveform of a compensating filter. Although the stress-to-charge transformation is very nonlinear, both the voltage distortion and restoration process are linear transformations. Superposition, and thus the convolution process, properly applies.

That correction filter, represented as a time-domain waveform, numerically convolved with the distorted stress record accurately produces the integral of the sensor output voltage that was applied at the measuring system input. The result is directly related to the stress-produced charge.

# Signal Prediction

## Charge-Mode Recording

The transient response of the stress-wave measurement is usually more limited by the associated electrical circuit than by the PVDF sensor characteristics.

For the charge mode, the load shunt resistance,  $R_\ell$ , is very large so that the voltage is observed "open circuit" across the load capacity,  $C_\ell$ , Figure 5. No integrator is required but the input impedance must be high; greater than  $10^{10} \Omega$  is commonplace. The high input impedance makes the measurement vulnerable to a variety of charge noise sources including triboelectric cable noise and IEMP (internal electromagnetic pulse). Cable capacitance must be stable. Nevertheless, the very high output possible with PVDF sensors often makes the signal-to-noise (S/N) ratio acceptable even under severe UGT conditions. Records of very high S/N ratios have been obtained under extreme noise conditions with other piezoelectric sensors.<sup>6c</sup>

The circuit serves as a capacitive voltage divider so that the voltage viewed across  $C_\ell$  is

$$V_\ell = \left( \frac{1}{C_s + C_c + C_i + C_r + C_\ell} \right) Q(t) . \quad (6)$$

## Current-Mode Recording

For the current mode, the current,  $i$ , through the current-viewing resistor (CVR) is

$$i = \frac{dQ}{dt} . \quad (7)$$

The corresponding voltage across the CVR,  $R_\ell$ , is

$$V_\ell = R_{cvr} \frac{dQ}{dt} . \quad (8)$$

The current-mode sensor output voltage across the CVR is related to the stress. If the power-law form of calibration expressed by Eq. (2) is used, the voltage in terms of stress is

$$V_\ell = R_{cvr} A a \frac{d}{dt} (\sigma^b) \quad (9)$$

where  $a$  and  $b$  are the two parameters of the power-law fit and  $A$  is the electrode area.

This demonstrates that the sensor voltage is proportional to the derivative of (approximately) the square root of stress rather than of stress directly as the exponent,  $b$  from Eq. (2), has a value of about 1/2.

These equations, the operations outlined in the Appendix, a relevant calibration such as the temporary one supplied in Eq. (2), and an adequate step-response characterization of the actual field measurement system provide the information required to properly apply the PVDF stress element. Both prediction of output and deduction of stress input can be accomplished with just these data.

## Example of Prediction and Deduction

The process from prediction of the voltage waveform to be recorded to the recovery of the input stress waveform is illustrated and validated by the following example. The stress waveform changes in several stages before being recorded as a voltage. Progressive calculation of the several intermediate waveforms is illustrated by Figures 8, 9, and 10.

## Prediction of Output Voltage

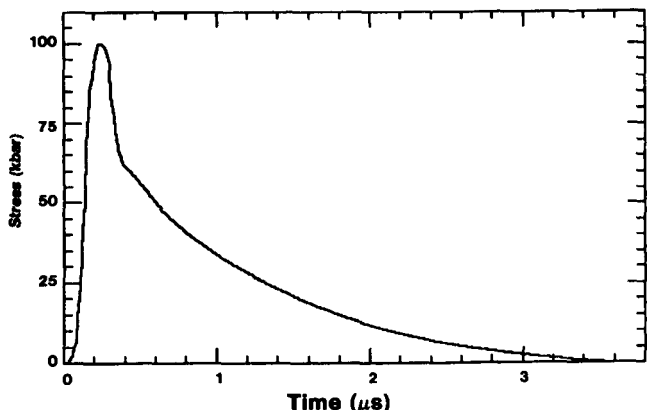
*Input Stress.* Figure 8(a) depicts a wave-code-predicted stress pulse for an actual field experiment. The waveform appears to be smooth with little structure.

*Charge Response.* The corresponding charge history calculated from Eq. (2) for a 3-mm-square stress element is given in Figure 8(b). The waveform has been noticeably modified, yet is recognizable.

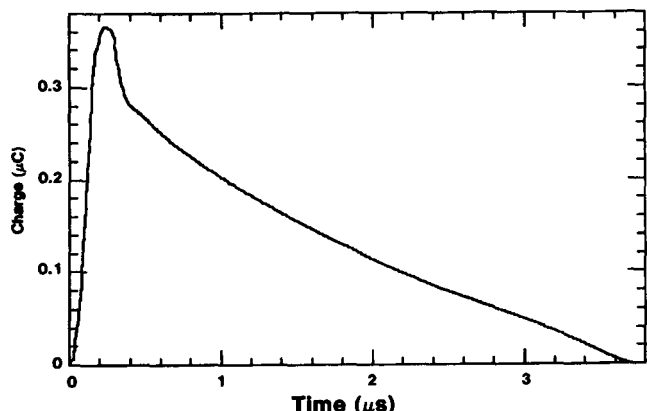
*Current Response.* However, in Figure 8(c) the calculated sensor output voltage as viewed across a 100- $\Omega$  CVR is entirely different. This is the form of sensor output that appears at the input of the long cable of the measuring system. The frequency content has been enriched in high frequencies and the voltage pulse does not resemble the stress pulse. Irregularities in the stress rate are made evident.

*Cable Response.* The imperfect response characteristics of components of the measuring system are shown in Figure 9. The voltage signal is conveyed through a 2000-ft-long (610 m) RG22 twinaxial cable that has the measured step response shown in Figure 9(a). This resembles a first-order exponential response but is more complex because the cable is a system of distributed resistances, capacitances, and inductances. The 2- $\mu$ s cable "rise time" is too long for faithful signal transmission.

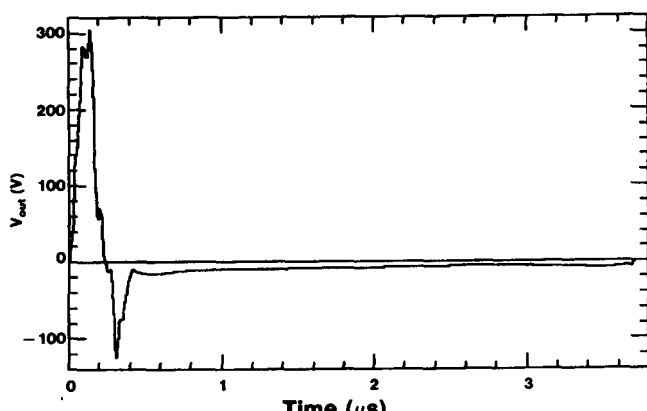
*Integrator Response.* The cable output voltage is input to an imperfect hardware integrator of a 2- $\mu$ s time constant. The step response of the actual RC "integrator" is shown in Figure 9(b). For the 3- $\mu$ s-duration stress signal, the integrator should have a time constant no shorter than 30  $\mu$ s.



(a) Wave-code-predicted input stress waveform



(b) Charge-mode charge response to stress



(c) Current-mode voltage output at sensor CVR

**Figure 8.** Waveform conversion from stress to charge to voltage

**Overall System Response.** The overall system step response predicted by convolution of the cable, “integrator,” and recorder responses as experimentally measured end to end in the system from cable input to the 100-MHz recorder output, is shown in Figure 9(c). Such a characterization should be performed on the actual recording system for each sensor.

**Ideal Integrator Response.** An ideal linear ramp output (the integral of the voltage input) is desired. Such a ramp, scaled to produce the integral of a voltage-step input to the system, is presented in Figure 9(e).

**Complementary Filter Response.** Figure 9(f) shows the step response of a complementary filter required to correct the data distorted by the cable and hardware integrator. The complementary filter, or compensator, characteristic was determined by the deconvolution of a “perfect” integrator characteristic waveform, Figure 9(e), with the overall system response, Figure 9(d). Slight truncation of the front end of the overall system response has been performed to allow stable deconvolution with the linear ramp to design the numerical compensating filter.

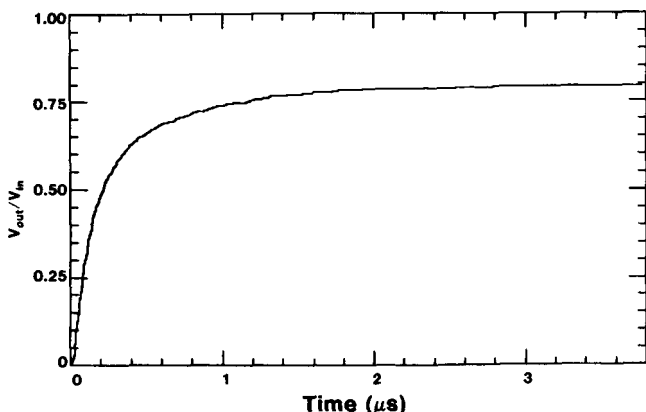
## Reduction of Recorded Voltage to Stress Input

**Charge Input.** The numerical complementary filter, Figure 9(f), produces an approximation of the charge input when convolved with the distorted voltage output, Figure 10(a). The result of the deconvolution of the recorded signal, Figure 10(a), with the complementary filter, Figure 9(e), scaled by the reciprocal of the value of the CVR, 100 Ω in this example, produced the input charge to the system, Figure 10(b).

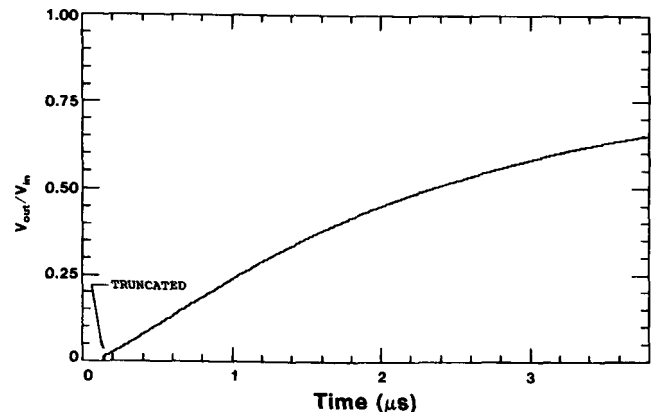
**Deduced Stress Input.** Because the power-law expression of calibration is simple, stress can be expressed as a direct function of charge by inversion of Eq. (2):

$$\sigma = 3.05 (Q/A)^{1.83} . \quad (10)$$

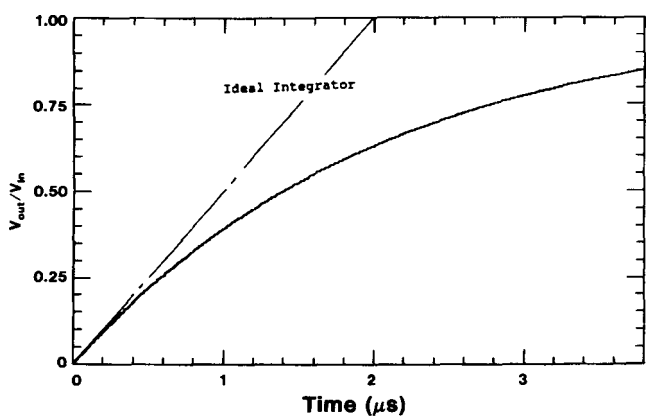
The sensor charge output waveform array, Figure 10(b), and sensor area are used in Eq. (10) to determine the stress input. The resulting waveform shown in Fig 10(c) is the stress input to the PVDF sensor as calculated from the predicted (or recorded) voltage record.



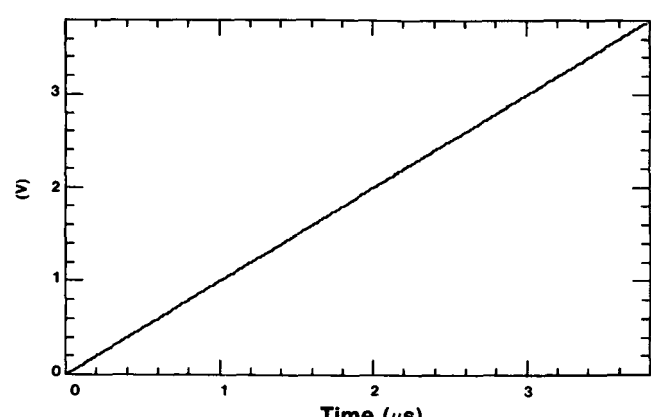
(a) Step response of 2000-ft RG22 cable



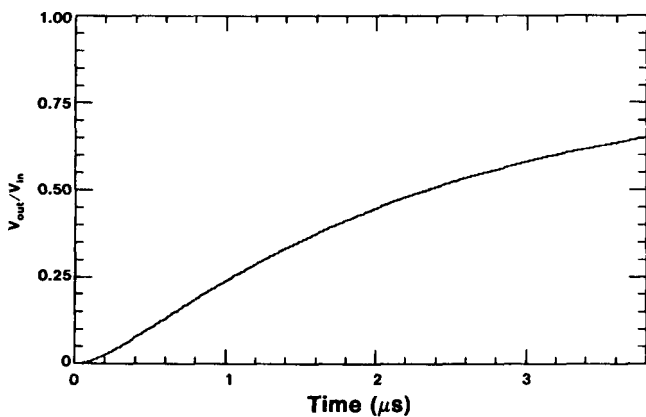
(d) End-to-end system step response (truncated)



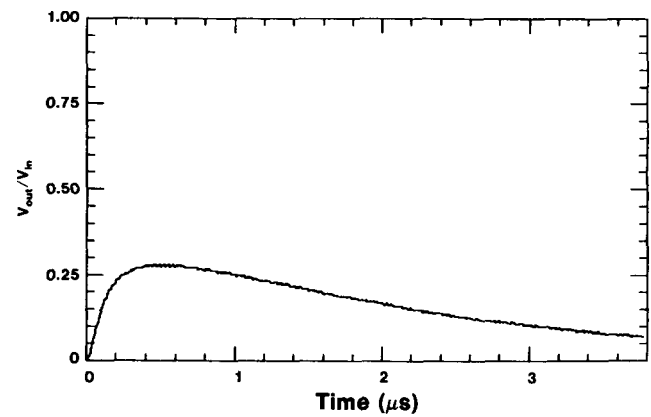
(b) Step response of imperfect RC "Integrator"



(e) Response of ideal integrator (numerical)

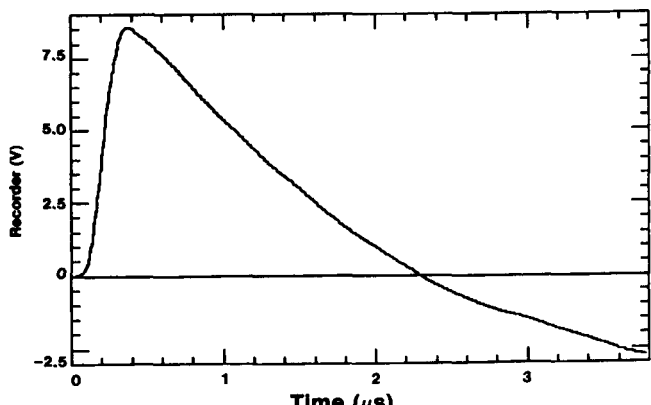


(c) End-to-end system step response

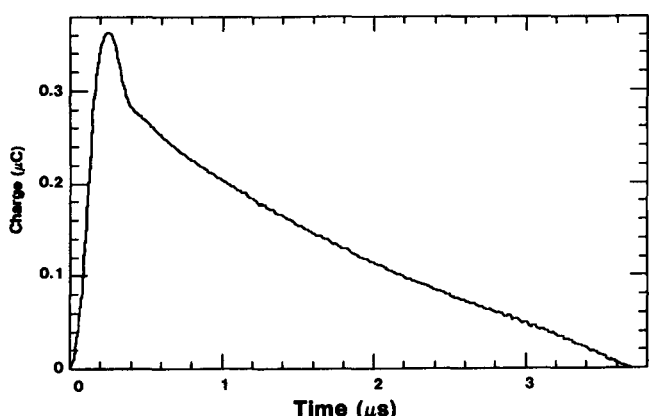


(f) Step response of complementary filter (numerical)

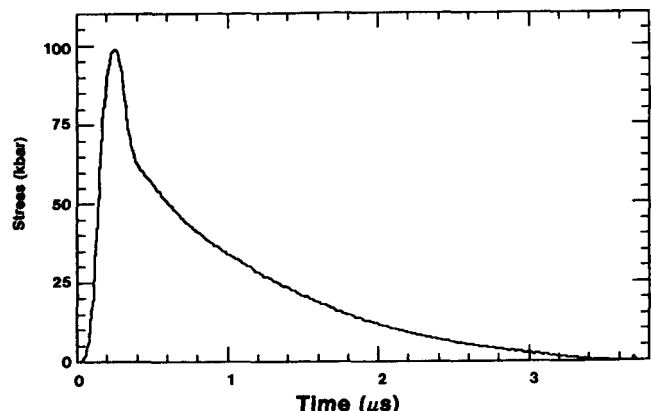
**Figure 9.** Voltage step response characteristics of the measuring system and its hardware and numerical components



(a) Distorted voltage predicted for recorder output



(b) Deduced charge output from sensor



(c) Deduced input stress to the sensor

Figure 10. Calculated input stress deduced from "recorded" voltage

## Significance of Example

Waveforms of Figure 10(c) and Figure 8(a) are practically the same. This illustrates that one can accurately determine the input stress to the sensor if care is taken in acquiring the data and determining the cable, hardware integrator, and recording system

overall step response for the actual measurement system. The initial stress input and the stress waveform deduced from the measurement agree in amplitude within 1%. This full-circle process—from predicted stress through distortion to deduced stress input—validates the mathematical process of data treatment for an exceptionally distorted recording. It does not account for the possible effect of error in the experimental determination of system or waveform characteristics.

The imperfections of the system were arbitrarily exaggerated in Figure 9 to emphasize the significant points. Nevertheless, the characteristics are entirely realistic. For a stress pulse of much shorter duration, say 200 ns, the integrator would be adequate. For a stress pulse of duration longer than 3 μs, the cable response would be adequate.

But, even with greatly exaggerated characteristics, the hybrid technique successfully recovered the initial stress input from a very distorted voltage output recorded by a system of inadequate characteristics.

In this realistic illustration, it is worth noting that the peak output from the small 3×3-mm sensor is 300 V at 3 A from the 100-kbar stress pulse. This is not unusual. In calibrating by precision projectile impact, peak currents of many amperes are experienced. The system and signal conditioning in this example have reduced the voltage to ~8.5 V maximum at the input to the recording system. The "integration," although imperfect, has produced a voltage output that is predictable, large, and of amplitude convenient for recording. Note, however, that the "recorded" waveform has been seriously distorted. Although the peak occurs at an appropriate time, the shape does not suggest the true structure of the stress pulse, and the duration appears to be shortened. The area of the waveform, often of interest for studies of impulse, is substantially affected. The amplitude of the pulse is much smaller than would have been predicted had the system distortion not been recognized.

Also, the recorded voltage waveform has developed a significant negative excursion not present in the input stress waveform. Bipolar voltage recording of the monopolar stress signal would have been required. Had the negative excursion not been predicted, an essential portion of the waveform would have been lost if the signal had been recorded only in an expected positive polarity. Prediction, using measured system characteristics, allows for proper scale-ranging of the recording.

In this hypothetical example, none of the distortion is due to faulty behavior of the PVDF sensing element. The distortion is a normal reproducible

result of inappropriate signal conditioning and of the authentic nonlinear calibration of the stress sensor.

The hybrid hardware-software measurement technique of recording and correction has been employed successfully in both UGT HLOS and VLOS experiments under severe measurement conditions. The pitfalls described are real and have been experienced by several experimenters under typical field test measurements conditions.

## Summary

The PVDF sensing element has already been studied in more careful detail than most contemporary shock-stress sensors (but much essential information remains to be learned!). The element makes possible an expanded range of measurement opportunities because of its exceptional sensitivity, accuracy, and versatility. It can be used in very different ways, each requiring distinctive approaches to signal conditioning and analysis. However, that very versatility demands that the user carefully understand the details of sensor and system behavior under a proposed circumstance of use. Properly used, the PVDF sensor is capable of high accuracy. But, careless or naive use of this capable standardized sensor without an understanding of, or a regard for, its unusual characteristics and requirements for signal conditioning can produce meaningless results, not merely slight inaccuracy. Unsatisfactory results tend improperly to discredit the valid sensor, but spurious results should not be casually blamed on the sensor itself.

Some of the principles and pitfalls of the use of the PVDF shock-stress sensing element in field measurement have been outlined, along with a novel hybrid hardware-software approach to integration and waveform distortion correction. General details are presented in classical technical references, and particular problems have been treated in greater detail in special publications cited in the references.

## References

<sup>1</sup>F. Bauer, "Behavior of Ferroelectric Ceramics and PVF<sub>2</sub> Polymers Under Shock-Loading," *Shock Waves in*

*Condensed Matter*, W. J. Nellis, L. Seaman, and R. A. Graham, Eds., American Institute of Physics, 1981.

<sup>2</sup>R. P. Reed, "Recent Developments in Piezoelectric Polymer Stress Gauges," *Proceedings, Range Commander's Council—14th Transducer Workshop, Colorado Springs, CO, 16-18 June 1987*.

<sup>3</sup>F. Bauer, "Method and Device for Polarizing Ferroelectric Materials," Patent 4611260, September 9, 1986.

<sup>4</sup>R. P. Reed, R. A. Graham, L. M. Moore, L. M. Lee, and F. Bauer, "Standard Specification for Piezoelectric Polymer Stress-Transducing Elements," Sandia National Laboratories report, in preparation (1989).

<sup>5</sup>A commercial line of PVF<sub>2</sub> shock-sensing elements is made using the Bauer process under license from ISL, by Metravib RDS, Ecully, France. The US distributor is Ktech Corporation, Albuquerque, NM.

<sup>6</sup>R. A. Graham and R. P. Reed, Eds., *Selected Papers on Piezoelectricity and Impulsive "Pressure" Measurement*, SAND78-1911 (Albuquerque, NM: Sandia National Laboratories, 1978).

- a. R. A. Graham, "Piezoelectric Current From Shunted and Shorted Guard-Ring Quartz Gauges," pp 91-99.
- b. R. P. Reed, "The Sandia Field Test Quartz Gage—Its Characteristics and Data Reduction," pp 149-175.
- c. R. P. Reed, "A System for Measurement of Free-Field Stress Waves Using Lithium Niobate Piezoelectric Transducers," pp 199-219.

<sup>7</sup>R. A. Graham, L. M. Lee, and F. Bauer, personal communication, 1987-88.

<sup>8</sup>R. A. Graham, F. Bauer, L. M. Lee, and R. P. Reed, "The Standardized Bauer Piezoelectric Polymer Shock Gauge," *Shock Wave Compression of Condensed Matter*, Proceedings of the Symposium in Honor of George E. Duvall held at Washington State University, Pullman, WA, September 1, 1988.

<sup>9</sup>M. U. Anderson and D. E. Wackerbarth, *Technique and Data Analysis for Impact-Loaded Piezoelectric Polymers (PVDF)*, SAND88-2327 (Albuquerque, NM: Sandia National Laboratories, November 1988).

# APPENDIX

## Numerical Methods

The proper treatment of PVDF data requires numerical differentiation, integration (quadrature), convolution (“folding”), and deconvolution (“unfolding”). Although these common fundamental math operations are well known to many users of PVDF data, they are not familiar to others who must work with the data. Moreover, the way in which these operations are numerically performed is quite varied. To avoid ambiguity in data analysis, the numerical method and the time-step and scaling relation should always be given with a result.

For the convenience of the reader, and to specifically define the simple tools as we currently use them in data analysis, the processes are described here for an arbitrary sampled waveform  $W(i)=W(1),W(2),\dots,W(N)$  known at uniform time intervals,  $Dt$ . Typically,  $W(1)=0$  and  $W(N)\neq 0$ .

### Numerical Differentiation

For the first and last points of a waveform, the derivative  $D(i)$  is

$$D(1) = [W(2) - W(1)]/Dt \quad \text{and} \quad (\text{A1})$$

$$D(N) = [W(N-1) - W(N)]/Dt, \text{ respectively.} \quad (\text{A2})$$

For other points, the derivatives are

$$D(i) = [W(i+1) - W(i-1)]/(2*Dt). \quad (\text{A3})$$

### Numerical Integration

For waveform analysis, it is the *progressive* time-dependent integral that is needed, not the *total* integral. Thus, accurate numerical integration is most conveniently performed on data sampled at uniform time steps. Where data are not digitized at uniform intervals, they must be repartitioned by interpolation. Arbitrary interpolation can introduce additional error, particularly in peak values.

For the first points of a waveform, the cumulative integral,  $I(i)$ , is

$$I(1) = I1 \text{ (generally } I1=0) \quad (\text{A4})$$

$$I(2) = Dt * [W(1) + W(2)]/2 + I(1). \quad (\text{A5})$$

For all other points, and particularly on ramp waveforms or linear segments,

$$I(i) = Dt * [W(i-1) + W(i)]/2 + I(i-1). \quad (\text{A6})$$

The above algorithm is the trapezoidal rule. It is exact for linear ramps and linear segments of waveforms.

For data sampled at intervals so that the waveform between sample points is significantly curved, a form that infers a parabolic arc fit between three adjacent points is more accurate (but it is less accurate for linear ramps). Thus, the parabolic alternative for points above  $i=2$  of significantly curved functions is generally

$$I(i) = Dt * [W(i-2) + 4*W(i-1) + W(i)]/3 + I(i-2). \quad (\text{A7})$$

Such algorithms are used by such microcomputer general-analysis codes as MathCad, View Point, and ASYST. They are very easily implemented in general-purpose spreadsheet analysis programs such as Quattro, VP Planner, and even Lotus 1-2-3. They, and the following algorithms, are easily programmed in any high-level language such as FORTRAN (or structured ANSI standard Full BASIC, similar to FORTRAN), PASCAL, or C.

More elaborate techniques are available; in particular, differentiation or integration of interpolating- or smoothing-cubic-spline representation of the data.

### Time-Domain Numerical Convolution

The classical mathematical operation of convolution is often performed by Laplace-, Fourier-, FFT-, Z-transform or other methods in a subsidiary transform domain (e.g., frequency). Many implementations of these tools are available and can be used.

Their use, however, involves many separate steps and, sometimes, the preliminary modification of the data sets.

A much simpler equivalent analysis employs the experimentally convenient step response as the system characterization and uses it in the time domain, as recorded. For short transient waveforms a simple algebraic recursion time-domain method—the classic Duhamel superposition method—directly equivalent to and derivable by the Z-transform is used. This process works very well. It is particularly effective in the interactive microcomputer analysis of waveforms of fewer than about 1024 points. Convolutions of 500 points can be performed in <4 min on an MS DOS 286 computer. An overall economy of time is gained by performing the operation directly in a single step rather than by the multi-step operation required by the frequency domain approach.

The simple algorithm, expressed in the recently standardized ANSI Full BASIC, is as follows:

```
R(1) = S(1) * W(1)

FOR N = 2 TO NPOINTS
    R(N) = S(1) * W(N)
    FOR M = 1 TO (N-1)
        R(N) = R(N) + (S(N-M+1)
                        - S(N-M)) * W(M)
    NEXT M
NEXT N
```

(A8)

The input waveform,  $W(i)$ , is convolved with the system-characterizing step-function response,  $S(i)$ , to predict the output response waveform,  $R(i)$ . The three arrays are sampled at the same times at uniform

intervals. The convolution operation is stable for all waveforms.

## Time-Domain Numerical Deconvolution

The mathematical inverse of the convolution is expressed by the recursive time-domain deconvolution algorithm:

```
W(1) = R(1)/S(1)
FOR N = 2 TO NPOINTS
    SUM = 0
    FOR M = 1 TO N-1
        SUM = SUM + (S(N-M+1)
                        - S(N-M)) * W(M)
    NEXT M
    W(N) = (R(N) - SUM)/S(1)
NEXT N
```

(A9)

Given the output response waveform,  $R(i)$ , and the system-characterizing step-response waveform,  $S(i)$ , this algorithm estimates the input waveform,  $W(i)$ . The deconvolution operation is potentially unstable.

Clearly,  $S(1)$  cannot be zero. In the usual circumstance where the step response begins with zero value and has a gradually rising "toe," a stable and very satisfactory estimate of  $W(i)$  can usually be made by truncating the first few points from the "toe" to the point where stability of the operation is attained. This truncation process may introduce a significant artificial time delay in the deconvolved data. That delay must be adjusted where differential break or arrival times between related waveforms are of interest.